LAWRENCE
LIVERMORE
NATIONAL
LABORATORY

LLNL-JRNL-646493

Modulation of medium pH by Caulobacter crescentus facilitates recovery from uranium-induced growth arrest

D. M. Park, Y. Jiao

November 19, 2013

Applied and Environmental Microbiology

Disclaimer

Modulation of medium pH by *Caulobacter crescentus* facilitates recovery from uranium-induced growth arrest

Running Title: U-induced growth arrest in *C. crescentus*

Dan M. Park[1], Yongqin Jiao[1]*

[1]Physical and Life Sciences Directorate, Lawrence Livermore National Laboratory, Livermore, CA 94550

*Corresponding Author. Phone: 925-422-4482. Fax: 925-422-2099. E-mail: jiao1@llnl.gov

Abstract

The oxidized form of uranium (U(VI)) predominates in oxic environments and poses a major threat to ecosystems. Due to its ability to mineralize U(VI), the oligotroph *Caulobacter crescentus* is an attractive candidate for U(VI) bioremediation. However, the physiological basis for U(VI) tolerance is unclear. Here we demonstrated that U(VI) caused a temporary growth arrest in *C. crescentus* and three other bacterial species, although the duration of growth arrest was significantly shorter for *C. crescentus*. During the majority of the growth arrest period, cell morphology was unaltered and DNA replication initiation was inhibited. However, during the transition from growth arrest to exponential phase, cells with shorter stalks were observed, suggesting a decoupling between stalk development and the cell cycle. Upon recovery from growth arrest, *C. crescentus* proliferated with a growth rate comparable to that of a no U(VI) control, although a fraction of these cells appeared filamentous with multiple replication start sites. Normal cell morphology was restored by the end of exponential phase. Cells did not accumulate U(VI) resistant mutations during the prolonged growth arrest, but rather, a reduction in U(VI) toxicity occurred concomitantly with an increase in medium pH. Together, these data suggest that *C. crescentus* recovers from U(VI)-induced growth arrest by reducing U(VI) toxicity through pH modulation. Our finding represents a unique U(VI) detoxification strategy and provides insight into how microbes cope with U(VI) under non-growing conditions, a metabolic state that is prevalent in natural environments.

Introduction

Depleted uranium (U) is a widespread environmental contaminant with major sources coming from energy and weapons production (1). The chemical toxicity of U poses a major threat to organisms and the environment. The extent of the environmental risk is dependent on the biogeochemical conditions that affect U

41 speciation and toxicity (1, 2). In the anoxic subsurface, U is usually present in the
42 reduced form U(IV) that is less toxic and less soluble compared to the oxidized form
43 U(VI). In contrast, in oxic surface waters, the highly toxic and mobile U(VI)
44 predominates (1). At circumneutral pH, U(VI) oxycations are present and form stable,
45 soluble complexes with carbonate, phosphate and natural organic matter, which greatly
46 influence the mobility and toxicity of U(VI) (1). The formation of these complexes is
47 governed by pH, redox potential, temperature, and ligand concentration (1, 3, 4).
48 Although the relationship between U(VI) speciation and bioavailability is complex since
49 certain ligands can either promote or inhibit U(VI) immobilization depending on the
50 environmental conditions, it is evident that U(VI) in strong complexes or adsorbed to
51 colloidal or particulate matter has reduced bioavailability and toxicity compared to the
52 naked U(VI) oxycation (1, 5). Given the high toxicity and bioavailability of U(VI), the
53 development of bioremediation strategies that reduce its mobility and bioavailability in
54 contaminated sites is of significant interest.
55 Microorganisms play an important role in governing U speciation and transport in
56 the environment and, thus, understanding the microbial factors that influence U
57 transformation is important in predicting U biogeochemical cycling and remediation
58 strategies (6). Extensive studies on U bioremediation in the past decades have
59 predominantly focused on the reduction of U(VI) to U(IV) by dissimilatory metal-reducing
60 bacteria under anaerobic conditions (7). Although less well studied under aerobic
61 conditions, microbes have been reported to detoxify and immobilize U(VI) through
62 surface adsorption, intracellular accumulation, and precipitation (6). In particular,
63 extracellular polysaccharides (EPS) secreted by many microorganisms contain side
64 groups with negatively charged ligands such as hydroxyl, carboxyl, or phosphate, which
65 attract cations like U(VI) and reduce their mobility (8, 9). Additionally, phosphatase

66 enzymes have been reported to mediate U(VI) precipitation through the release of
67 inorganic phosphate from organophosphates (10-14).
68 The ubiquitous aerobe *Caulobacter crescentus* holds promise for U(VI)
69 bioremediation because of its ability to mineralize U(VI) and survive in low-nutrient
70 environments (15, 16). The recent isolation of heavy metal resistant *Caulobacter*
71 species from sites contaminated with heavy metals further highlights the environmental
72 relevance of this genus (17, 18). *C. crescentus* undergoes an asymmetric cell division
73 that yields two daughter cells with differing morphological and regulatory features (19).
74 This includes a motile, chemotactic swarmer cell and a stalked cell that contains a thin
75 cylindrical protrusion of the cell envelope (stalk). Stalked cells are able to reinitiate cell
76 division, whereas swarmer cells must differentiate into stalked cells in order to divide.
77 The distinct cell cycle-associated morphological features in *C. crescentus* allow
78 examination of the effect that U(VI) exerts on cell cycle processes. Despite its high
79 tolerance and environmental relevance, little is known about the physiology and
80 detoxification mechanisms of *C. crescentus* with respect to U(VI). Recently, we showed
81 that extracellular phosphatase activity mediated by PhoY is critical for survival in media
82 containing organophosphates and U(VI) (14). In this study, we characterized the
83 temporary growth arrest response employed by *C. crescentus* during exposure to U(VI)
84 and identified a unique U(VI) detoxification strategy.
85 **Materials and Methods**
86 **Bacterial strains and growth conditions.** *Caulobacter crescentus* NA1000,
87 *Escherichia coli* K12, *Pseudomonas aeruginosa* PAO1, and *Pseudomonas putida*
88 KT2440 were used in this study. Growth experiments were performed in 1) PYE
89 medium, containing 0.2% (wt/vol) Bacto peptone (Difco), 0.1% yeast extract (Difco), 1
90 mM $MgSO_4$ and 0.5 mM $CaCl_2$, 2) phosphate buffered minimal medium (M2G) (20), or 3)
91 modified M5G medium (21) supplemented with 5 mM glycerol-2-phosphate in place of

92 inorganic phosphate. Cultures were grown at 30°C with shaking to mid-exponential
93 phase prior to use in experiments. Unless otherwise specified, an inoculum size of 9 x
94 10^7 cells/ml was used in all *C. crescentus* experiments.
95 **Uranium toxicity experiments.** Uranyl nitrate hexahydrate [$(UO_2)(NO_3)_2$*$6H_2O$;
96 hereafter, U(VI)] was obtained from SPI Supplies (West Chester, PA) and 100 or 200
97 mM stock solutions were prepared in 0.1 N nitric acid followed by filtration through a
98 0.22-µm membrane. The U(VI) concentration of the stock solution was confirmed by
99 Inductively coupled plasma mass spectrometry (ICP-MS). Spontaneous U(VI)
100 precipitation was observed upon addition of uranyl nitrate to PYE with a maximum
101 solubility of ~75 µM. The U(VI) concentrations described in the text correspond to the
102 initial added U(VI); solubility measurements at each added U(VI) concentration are
103 shown in Fig. S1. The pH of each growth medium including those lacking added uranyl
104 nitrate was standardized through the addition of an equivalent amount of HNO_3. Where
105 indicated, the supernatant from cell cultures was collected by centrifugation at 20,000 x
106 *g* for 8 min then filtered through a 0.22-µm membrane. Heat-killed cells were prepared
107 by incubation at 70°C for 15 min followed by colony forming units (CFU) measurements
108 and propidium iodide staining to confirm treatment efficacy and phase contrast
109 microscopy to confirm cell integrity. The optical density at 600 nm (OD_{600}) was
110 determined using a BioTek Synergy H1 Microplate Reader. CFU were determined by
111 diluting and plating on PYE agar.
112 Cells were synchronized as described previously (22). Briefly, exponential phase
113 cells were resuspended in 10 mM phosphate buffer, pH 7.0, added to an equal volume
114 of Percoll (Pharmacia) and centrifuged at 10,000 × *g* for 20 min at room temperature.
115 The lower swarmer band was removed, washed twice with the phosphate buffer and
116 resuspended in PYE.

To compare the effect of U(VI) on growth of *Escherichia coli* K12, *Pseudomonas aeruginosa* PAO1, and *Pseudomonas putida* KT2440 to that of *C. crescentus*, cells grown to mid-exponential phase (OD_{600} ~0.25) in PYE were washed once in PYE to remove the spent medium and inoculated into PYE containing 350 μM U(VI). Since growth recovery was dependent on metabolic activity, the inoculum was normalized by biomass, as determined by cell dry weight (Table S1). The cell dry weight was determined by growing all strains to an OD_{600} of 0.5, centrifuging at 20,000 x *g* for 8 min, washing twice in 1x phosphate buffered saline (PBS, pH 7), and drying overnight at 65°C. There was less than a three-fold difference in cell number among the four strains after normalization by biomass (Data not shown).

Assays of U(VI) concentration. The U(VI) concentration was determined spectrophotometrically using the Arsenazo III reagent (23). A 1% (w/v) Arsenazo III stock solution was prepared in 6.25% (w/v) trichloroacetic acid (TCA) and filtered with a 0.22-μm membrane. To measure the soluble U(VI) concentration, samples were centrifuged at 20,000 x *g* for 5 min at room temperature and 40 μl of supernatant was acidified with an equal volume of 12.5% (w/v) TCA before the addition of 60 μl Arsenazo III stock solution and the absorbance at 652 nm was measured. Total U(VI) concentration was determined as described above, except an equal volume of 12.5% (w/v) TCA was added before centrifugation. The U(VI) concentration was calculated using a standard curve.

β-galactosidase assays. NJH199 (24), a NA1000 derivative lacking CC_1634 (*lacA*) and containing a plasmid-borne translational P_{urcA}-*lacZ* fusion, was grown in PYE containing U(VI) in the presence of 2 μg/mL chloramphenicol. This reporter fusion included a 1 kb region upstream of the *urcA* start codon through the first 24 nucleotides of *urcA,* fused to *lacZ* (24). To terminate cell growth and any further protein synthesis,

142 tetracycline was added to a final concentration of 1 µg/ml and cells were placed on ice.
143 β-galactosidase activity was assayed as previously described (25).
144 **Fluorescence microscopy.** The membrane potential probe bis-(1,3-dibutylbarbituric
145 acid) trimethine oxonol ($DIBAC_4(3)$; Molecular Probes, Inc), that enters cells with
146 depolarized membranes, and the dead cell stain propidium iodide ReadyProbes (PI;
147 Molecular Probes, Inc) were used to assess cell viability during growth arrest induced by
148 350 µM U(VI). $DIBAC_4(3)$ was added at 1 µg/ml and PI was used according to the
149 manufacturers instructions. After dye addition, samples were incubated for 30 min at
150 30°C, concentrated by 10-fold, then immobilized using a thin layer of PYE-agarose.
151 Phase contrast and fluorescence microscopy images were obtained using a Leica DMI
152 6000B microscope with an HCX PL APO 63×, 1.40 numerical aperture, oil PH3 CS
153 objective, and a Leica DFC360 FX camera. Fluorescein isothiocyanate (FITC) and
154 rhodamine filters were used for $DIBAC_4(3)$ and PI, respectively.
155 MT190 (26), a NA1000 derivative with a *ecfp-parB* fusion in place of the
156 chromosomal copy of *parB*, was synchronized as described above and inoculated into
157 PYE containing 350 µM U(VI). At different time points, cells were fixed in 4%
158 formaldehyde in 1x PBS buffer (pH 7) for 30 min at room temperature and the U(VI)
159 precipitates were solubilized with 1M $NaHCO_3$ (pH 8.5) (27). Cells were washed with 1x
160 PBS, spotted onto a 1% agarose pad and imaged using an Axiovert 200M microscope
161 (Zeiss, Minneapolis, MN) equipped with a Photometric CoolSNAP HQ CCD camera.
162 Images were acquired with a 100x DIC objective and an eCFP filter set (Chroma,
163 Bellows Falls, VT). Images were processed using ImageJ (28) and fluorescent foci were
164 counted manually.
165 **Scanning electron microscopy.** Samples were fixed and U(VI) precipitates were
166 solubilized with bicarbonate as described above. Fixed cells were washed four times

with ddH_2O and allowed to dry overnight onto a silicon wafer. Scanning electron microscopy (SEM) images were taken with a JEOL JSM 7401-F FESEM instrument.

Results

U(VI) induces a reversible growth arrest in *C. crescentus*. The effect of U(VI) on the growth of *Caulobacter crescentus* NA1000 was determined in PYE with exponential phase cells as inoculum. U(VI) concentrations are reported as total added U(VI). U(VI) caused a temporary growth arrest that delayed the onset of exponential growth in a U(VI) concentration dependent manner (Fig. 1A). No growth recovery with U(VI) concentrations at or above 500 μM was observed after two weeks (data not shown). At a fixed U(VI) concentration (300 μM), the length of growth arrest was also dependent on initial cell density, with lower inoculum sizes extending the growth arrest duration (Fig. 1B). Below ~7 x 10^5 cells/ml, no growth recovery was observed, suggesting that there is a minimal cell density required for growth recovery (data not shown). Growth arrest was observed regardless of the growth phase of the inoculum (Fig. S2A), suggesting that U(VI) exposure arrested growth rather than extending a normal lag phase. Furthermore, direct addition of U(VI) to mid-exponential phase cultures induced growth arrest, but required higher U(VI) concentrations than when U(VI) was introduced during inoculation (Fig. S2B). After recovery from growth arrest, *C. crescentus* achieved the same growth rate and approximate final cell density as the no U(VI) control (Fig. 1). Thus, it appears that either *C. crescentus* has accommodated the U(VI) stress and/or the U(VI) toxicity was greatly reduced during growth arrest.

Colony forming unit (CFU) measurements during the course of growth arrest indicated that cell viability is dependent on U(VI) concentration. At 350 μM or lower, there was no change in cell viability throughout growth arrest (Fig. 1C). Dead cell staining with either propidium iodide or bis-(1,3-dibutylbarbituric acid) trimethine oxonol (DIBAC4(3)) indicated that greater than 99% of cells remained alive, suggesting that the

193 lack of a change in CFU is a result of growth arrest rather than equivalent rates of cell
194 growth and death (data not shown). Furthermore, the lack of DIBAC4(3) staining
195 suggests that the membrane remained polarized (29), indicative of a metabolically active
196 state. However, a decrease in viability is evident with U(VI) at or above 400 μM (Fig.
197 1C). The CFU count dropped approximately 25-fold at 400 μM U(VI) before growth
198 recovery, while no detectable viability (<10 CFU/ml) was observed at 500 μM U(VI) after
199 24 h (data not shown). This reduction in cell viability at higher U(VI) concentrations
200 provides a likely explanation for why a small increase in U(VI) concentration
201 disproportionally lengthens the duration of growth arrest as shown in Fig. 1A. Since 350
202 μM U(VI) elicits growth arrest without affecting viability, it was used to induce growth
203 arrest in the sections below, unless specified otherwise.
204 **Growth arrest is not specific to *C. crescentus*.** To determine whether the temporary
205 growth arrest response is specific to *C. crescentus*, the effect of U(VI) on the growth of
206 *Escherichia coli* K12, *Pseudomonas aeruginosa* PAO1, and *Pseudomonas putida*
207 KT2440 was tested. Exposure to U(VI) (350 μM) caused growth arrest in all species
208 tested, although the duration of growth arrest was different among species (Fig. 2). *P.*
209 *aeruginosa* and *P. putida* entered exponential phase after ~35 h and ~75 h of growth
210 arrest, respectively, which was significantly longer compared to *C. crescentus* (~8 h). *E.*
211 *coli* was the most sensitive to U(VI) as no growth recovery was evident after two weeks;
212 growth recovery was observed with a U(VI) concentration of 150 μM or lower (data not
213 shown). These data suggest that *C. crescentus* is more resistant to U(VI) than the other
214 three species tested, consistent with previous observations (16). The temporary growth
215 arrest observed for all four species tested suggests that stress-induced growth arrest
216 may be a common mode of U(VI) toxicity among aerobic bacteria.
217 **U(VI) inhibits swarmer to stalked cell progression.** To determine whether the
218 morphology of *C. crescentus* was altered during growth arrest, we visualized cells using

219 scanning electron microscopy (SEM). Compared to exponential phase cells prior to
220 U(VI) addition, no gross morphological changes or accumulation of any particular cell
221 type was observed during the first 4 h of growth arrest (Fig. 3A). Cells with shorter
222 stalks were observed towards the end of growth arrest (7 h), suggesting that U(VI) may
223 affect stalk development. To further test this notion, isolated swarmer cells were
224 exposed to U(VI) and visualized by SEM (Fig. 3B). No detectable morphological
225 changes were observed within the first 5 h of growth arrest, indicating that stalk
226 development was inhibited. During the transition to exponential phase, cells that had
227 reached the predivisional stage either appeared to completely lack stalks or possessed
228 abnormally short stalks, consistent with the results from un-synchronized cells. It should
229 be noted that swarmer cells exhibited a slightly longer growth arrest (by ~2 h) compared
230 to a mixed population (Data not shown), which may reflect the additional time required
231 for the initial swarmer to stalked cell transition and recovery from the added stress of the
232 synchronization procedure.
233 To determine whether chromosome replication initiation, which occurs
234 concomitantly with the swarmer to stalked cell transition, was also inhibited by U(VI),
235 synchronized cells containing a ParB-CFP fusion (26) were monitored throughout growth
236 arrest (Fig. 3C). ParB binds to *parS* sites in close proximity to the origin of replication
237 and is involved in chromosome partitioning. After replication initiation, the new origin is
238 moved to the opposite pole so *oriC* can be quantified by examining ParB-CFP foci within
239 a cell (30). Within the first 8 h of growth arrest, there was no change in the number of
240 cells with two parB-CFP foci, suggesting that U(VI) either inhibited chromosome
241 replication initiation or segregation (Fig. 3C). In contrast, 67% of cells inoculated in
242 media lacking U(VI) had two fluorescent foci after 1 h (Fig. 3D). Taken together, these
243 data suggest that U(VI) blocks the G1 to S transition of the *C. crescentus* cell cycle.

Interestingly, shortly after cells had transitioned into exponential phase (OD_{600} of 0.2), approximately 15% of the population appeared filamentous (Fig. 3A-B). The filamentous cells possessed multiple ParB-CFP foci, indicative of DNA replication without subsequent cell division (Fig. 3E). Although bacterial filamentation can arise from several different stresses (31), it is commonly associated with DNA damage and likely indicates cell division inhibition. Normal cell morphology was restored by the end of exponential phase (Fig 3B).

Pre-exposure to U(VI) does not increase the ability to cope with subsequent U(VI) exposure. As a first step to deduce the mechanism that leads to growth recovery, we tested whether growth recovery of *C. crescentus* is a result of a beneficial mutation that confers U(VI) resistance. Cells grown on U(VI)-containing agar plates did not show increased viability compared to naïve cells when regrown on U(VI)-containing plates (Fig. 4A). Additionally, exponential phase cells that had recovered from U(VI)-induced growth arrest were not more resistant to U(VI), compared to cells without previous U(VI) exposure; both cultures experienced the same length of growth arrest when re-inoculated into U(VI)-containing media (Fig. 4B). Thus, pre-exposure to U(VI) did not shorten the duration of growth arrest. These data suggest that growth recovery is not caused by acquired mutations that confer U(VI) resistance. Furthermore, the retained U(VI) sensitivity in recovered cells suggests that if recovery from growth arrest is a result of altered gene/protein expression that confers U(VI) resistance, such changes are not preserved after growth recovery. This failure of pre-exposure to elicit enhanced U(VI) resistance is in contrast to other metals (*e.g.*, Cd) and toxic chemicals (*e.g.*, H_2O_2) where inducible detoxification pathways are responsible for resistance (32, 33). Recovery from growth arrest may, therefore, be a result of U(VI) detoxification rather than accommodation.

***C. crescentus* reduces U(VI) toxicity during growth arrest.** To evaluate the possibility that *C. crescentus* recovers from growth arrest by reducing U(VI) toxicity, the supernatant from a *C. crescentus* culture at the end of U(VI)-induced growth arrest was collected and used as growth media. Upon re-inoculation, the supernatant did not elicit growth arrest, but instead yielded growth kinetics identical to the no U(VI) control (Fig. 5A). In contrast, growth arrest was evident with supernatant collected from heat-killed cells or an abiotic control incubated with U(VI) for the same period of time, indicating that U(VI) detoxification is a physiological process. The heat-killed cells served to control for any process that may reduce U(VI) toxicity that is metabolism independent (*e.g.*, cell surface sorption). To further characterize this reduction in U(VI) toxicity, an aliquot of supernatant was extracted every ~75 min during growth arrest and re-inoculated with fresh *C. crescentus* cells. The time required for these cultures to reach mid-exponential phase (OD_{600} of 0.2), termed growth time, was measured. The growth time was inversely proportional to the amount of time that the supernatant had been exposed to *C. crescentus* during growth arrest (Fig. 5B). In other words, supernatant extracted from later time points of growth arrest was less toxic to cells. In contrast, no reduction in growth time was observed for the supernatant collected from an abiotic control. Thus, *C. crescentus* reduced the toxicity of U(VI) throughout growth arrest.

To further examine the reduction in U(VI) toxicity during growth arrest, the expression of P_{urcA}, a promoter that was previously shown to specifically sense U(VI) (24), was monitored using a plasmid-borne translational fusion of the first 8 AA of UrcA to LacZ under the control of the *urcA* promoter. Strikingly, the dynamics of P_{urcA}-*lacZ* expression correlated precisely with the duration of growth arrest (Fig. 5C). The expression of the P_{urcA}-*lacZ* reporter increased sharply during the initial period of growth arrest and reached a maximum towards the end of growth arrest. The reporter activity declined immediately upon growth recovery and returned to basal levels during

exponential phase, likely due to cessation of further P_{urcA}-*lacZ* expression and protein turnover and dilution during cell division. This result suggests that the U(VI)-induced stress sensed by P_{urcA} has been eliminated during growth arrest, consistent with the observed reduction in U(VI) toxicity.

U(VI) toxicity is reduced by modulation of medium pH through metabolic activity. Since pH is known to control U(VI) speciation and hence U(VI) toxicity (1), we monitored the medium pH. With 350 μM U(VI), *C. crescentus* increased the medium pH by approximately 0.4 units during growth arrest (from 5.7 to 6.1; Fig. 6A). The medium pH continued to increase throughout growth, reaching ~8.1 by early stationary phase. This increase was dependent on metabolic activity since no pH change was observed over the same time period when sodium azide, an inhibitor of cytochrome oxidase, was present (Data not shown). It should be noted that in the absence of U(VI) cell growth was not altered within this pH range (Fig. S3A) and medium alkalinization occurred throughout *C. crescentus* growth (data not shown). Medium alkalinization has frequently been noted during *E. coli* growth in LB and is attributed to ammonia excretion during amino acid catabolism (34). To test whether the observed pH increase was responsible for alleviating U(VI) toxicity, the pH of the U(VI)-containing growth medium (pH 5.7) was artificially increased to 6.1, the measured value at the end of growth arrest, prior to inoculation. Growth arrest was significantly shortened and P_{urcA} expression was greatly reduced as compared to a control with no pH adjustment (Fig. 6B-C). The metabolism-dependent modulation of medium pH and hence U(VI) toxicity provides a likely explanation for the observed effect of inoculum size on growth arrest duration; one would expect a larger size inoculum to increase pH at a faster rate.

To test whether pH modulation was also responsible for growth recovery in other bacterial species, we monitored the medium pH during growth in U(VI) for *E. coli*, *P. aeruginosa*, and *P. putida* (Fig. 6D). We note that lower U(VI) concentrations were

chosen for *E. coli* and *P. putida*, because of their high sensitivity towards U(VI). All three strains increased medium pH during growth arrest. Compared to *C. crescentus*, a higher pH (~6.5 compared to 6.1) was reached for these species before growth recovery was observed, consistent with the higher U(VI) tolerance observed for *C. crescentus*. Medium alkalinization was not observed for *E. coli* at 350 μM U(VI), consistent with the lack of growth recovery (data not shown). Importantly, pH adjustment also shortened the growth arrest duration of these three species (Data not shown), suggesting that pH modulation may be a general U(VI) detoxification mechanism.

To determine whether the pH increase affected U(VI) solubility, we monitored the soluble U(VI) concentration during the course of growth arrest for *C. crescentus* (Fig. 6E). It should be noted that spontaneous U(VI) precipitation was evident upon addition of U(VI) to the PYE growth medium, independent of the presence of cells. These U(VI) precipitates were not responsible for the observed U(VI) toxicity, since growth arrest was still observed upon their removal by centrifugation (Fig 5A). The solubility of U(VI) increased slightly during growth arrest at a rate that was indistinguishable from an abiotic control (Fig. 6E). Artificially increasing the growth medium pH from 5.7 (pH at the beginning of growth arrest) to 6.1 (pH towards the end of growth arrest) did not significantly affect U(VI) solubility (Fig. S3B). Together, our data point towards a pH-mediated detoxification mechanism that does not involve a change in U(VI) solubility.

U induces a similar reversible growth arrest in minimal media. Attempts to characterize the effect of U(VI) on *C. crescentus* growth in minimal media were made taking into account U(VI) solubility and phosphate limitation issues. Although M2G (20) is commonly employed as the defined minimal medium for *C. crescentus*, the limited solubility of U(VI) (~10 μM) in this phosphate buffered medium precluded phenotypic determination of U(VI) toxicity. Chelation with a 10:1 molar ratio of citrate or bicarbonate to U(VI) did not increase U(VI) solubility in M2G (data not shown). Furthermore,

phosphate limitation resulting from abiotic U-Pi precipitation hindered the use of low phosphate minimal media (*e.g.*, M5G (21)). Nevertheless, we found that the increased range of U(VI) solubility in modified M5G (M5G-G2P), where inorganic phosphate was replaced by glycerol-2-phosphate, allowed growth to be characterized. Similar to PYE, U(VI) caused a reversible growth arrest in M5G-G2P in a concentration dependent manner (Fig. S4A). In contrast to PYE, the soluble U(VI) concentration decreased during growth arrest (Fig. S4B), due to precipitation with Pi released from G2P through cellular phosphatase activity (14). Since the soluble Pi concentration remained low throughout growth arrest (Fig. S4C), a contribution of Pi limitation to the growth arrest cannot be excluded. Further work is underway to explicate the toxic effect of U(VI) in minimal media and to further characterize the mechanism of U(VI)-induced cell cycle arrest.

Discussion

Here, we demonstrated that in the presence of U(VI), *C. crescentus* entered a reversible, non-replicative state that was maintained until U(VI) was sufficiently detoxified. Metabolic activity during growth arrest increased growth medium pH, detoxified U(VI), and facilitated growth recovery. A loss of viability was observed during prolonged growth arrest periods with high U(VI) concentrations (>350 μM), highlighting the importance of U(VI) detoxification for cell survival. Growth recovery was not observed below a certain threshold inoculum size, indicating that there is a minimal quorum of *C. crescentus* required to overcome U(VI) toxicity. Together this data points towards a community-driven U(VI) detoxification process.

Growth recovery was marked by proliferation with normal growth kinetics but sustained susceptibility to U(VI), arguing against accumulation of U(VI) resistant mutants. Antimicrobial compounds such as heavy metals and antibiotics are common causes of growth arrest in microorganisms (32, 35-38). In many cases, recovery from

373 growth arrest is attributed to the induction of a genetically encoded resistance
374 mechanism or the selection of antimicrobial tolerant mutants during antimicrobial
375 exposure (32, 36). However, recent studies of microbial antibiotic resistance suggest
376 that resistance can stem from a reduced growth rate, which significantly diminishes the
377 potency of antibiotics (39). Our results indicate that *C. crescentus* is inherently
378 susceptible to and phenotypically tolerant of U(VI) in a similar manner. In accordance
379 with our data, substantial degradation of cellular RNA was observed when
380 *Metallosphaera sedula* was exposed to U(VI), suggesting that critical cellular processes
381 were aborted as a dynamic mechanism for resisting U(VI) toxicity (40). Thus, the
382 temporary growth arrest observed for *C. crescentus* may represent a survival strategy
383 against U(VI) toxicity.

384 The cellular and morphological changes observed during U(VI) exposure indicate
385 a disruption of the cell cycle. *C. crescentus* exposed to high levels of U(VI) arrested cell
386 cycle progression; the stalked cell transition and the initiation of DNA replication were
387 blocked in swarmer cells while cell division was inhibited in stalked and predivisional
388 cells. Recent proteomic analysis indicated that the levels of two master cell cycle
389 regulators, CtrA and DnaA, were significantly reduced during U(VI) exposure (41).
390 During the *C. crescentus* cell cycle, the abundance of these regulators is tightly
391 controlled in order to precisely regulate the timing of DNA replication. DnaA is required
392 for replication initiation (42) and CtrA inhibits replication in swarmer cells (43) but also
393 acts as a transcription factor for ~100 genes critical for cell cycle progression (44).
394 Down-regulation of DnaA and CtrA has been observed under conditions that cause cell
395 cycle arrest (*e.g.*, carbon starvation) (42). Thus, it is conceivable that U(VI)-induced cell
396 cycle arrest is at least in part a consequence of CtrA and DnaA depletion, although the
397 precise nature of the U(VI)-induced cellular stress and how it leads to cell cycle
398 disruption remain to be determined.

The finding that growth arrest is alleviated through alkalinization of the growth medium highlights the importance of pH in U(VI) toxicity. Given that U(VI) speciation is strongly influenced by pH in aquatic systems (1) and the absence of a pH-mediated change in U(VI) solubility during growth arrest, we speculate that U(VI) detoxification during growth arrest was a result of altered U(VI) speciation. It is generally accepted that the uncomplexed uranyl ion is the most toxic and bioavailable form of U(VI) while chelation with ligands such as phosphate, carbonate and organic acids reduces U(VI) toxicity (1). Previous studies suggest that an increase in pH within a range of 5-6 decreases U(VI) bioavailability by lowering the uranyl concentration in aquatic environments (45, 46). Consistently, U(VI) complexation by organic or inorganic phosphate was shown to reduce U(VI) toxicity in *C. crescentus* (14), while lower pH conditions that favor the presence of the uncomplexed uranyl ion appear more toxic to bacteria (47). Further analytical techniques will be required to substantiate a speciation dependency of U(VI) toxicity in our system.

In conclusion, we have demonstrated that U(VI) causes a reversible growth arrest in *C. crescentus*, with growth recovery mediated through a metabolism-dependent increase in medium pH. This detoxification mechanism is not specific to *C. crescentus*, suggesting that it may be a general mechanism of U(VI) defense by aerobic bacteria. Together, our results provide insight into how microbes cope with (metal) stress under non-growing conditions that are prevalent in the natural environment and highlight the need to consider the non-growing state, not simply active growing cells, when predicting microbial behaviors or planning a bioremediation system.

Acknowledgements

We thank Ping Hu, Yun Wang, Grant Bowman, Lucy Shapiro and Harley McAdams for generously providing the strains used in this study. We thank Fang Qian for her assistance with SEM. We thank Mimi Yung and Grant Bowman for providing critical

review of this manuscript. This work was performed under the auspices of the U.S. Department of Energy by Lawrence Livermore National Laboratory under contract DE-AC52-07NA27344 (LLNL-JRNL-646493). Funding was provided by a Department of Energy Early Career Research Program award from the Office of Biological and Environmental Sciences (to Y.J.).

References

1. **Markich SJ.** 2002. Uranium speciation and bioavailability in aquatic systems: an overview. The Scientific World Journal **2:**707-729.
2. **Gadd GM.** 2010. Metals, minerals and microbes: geomicrobiology and bioremediation. Microbiology **156:**609-643.
3. **Handley-Sidhu S, Worsfold PJ, Livens FR, Vaughan DJ, Lloyd JR, Boothman C, Sajih M, Alvarez R, Keith-Roach MJ.** 2009. Biogeochemical Controls on the Corrosion of Depleted Uranium Alloy in Subsurface Soils. Environmental science & technology **43:**6177-6182.
4. **Mishra S, Maity S, Pandit GG.** 2012. Estimation of distribution coefficient of natural radionuclides in soil around uranium mines and its effect with ionic strength of water. Radiation protection dosimetry **152:**229-233.
5. **Fortin C, Dutel L, Garnier-Laplace J.** 2004. Uranium complexation and uptake by a green alga in relation to chemical speciation: the importance of the free uranyl ion. Environmental toxicology and chemistry / SETAC **23:**974-981.
6. **Merroun ML, Selenska-Pobell S.** 2008. Bacterial interactions with uranium: an environmental perspective. J Contam Hydrol **102:**285-295.
7. **Wall JD, Krumholz LR.** 2006. Uranium reduction. Annual review of microbiology **60:**149-166.
8. **Macaskie LE, Yong P, Doyle TC, Roig MG, Diaz M, Manzano T.** 1997. Bioremediation of uranium-bearing wastewater: biochemical and chemical factors influencing bioprocess application. Biotechnology and Bioengineering **53:**100-109.
9. **Pal A, Paul AK.** 2008. Microbial extracellular polymeric substances: central elements in heavy metal bioremediation. Indian Journal of Microbiology **48:**49-64.
10. **Renninger N, Knopp R, Nitsche H, Clark DS, Keasling JD.** 2004. Uranyl precipitation by Pseudomonas aeruginosa via controlled polyphosphate metabolism. Applied and environmental microbiology **70:**7404-7412.
11. **Martinez RJ, Beazley MJ, Taillefert M, Arakaki AK, Skolnick J, Sobecky PA.** 2007. Aerobic uranium (VI) bioprecipitation by metal-resistant bacteria isolated from radionuclide- and metal-contaminated subsurface soils. Environmental microbiology **9:**3122-3133.
12. **Nilgiriwala KS, Alahari A, Rao AS, Apte SK.** 2008. Cloning and overexpression of alkaline phosphatase PhoK from *Sphingomonas* sp. strain BSAR-1 for bioprecipitation of uranium from alkaline solutions. Applied and environmental microbiology **74:**5516-5523.
13. **Merroun ML, Nedelkova M, Ojeda JJ, Reitz T, Fernandez ML, Arias JM, Romero-Gonzalez M, Selenska-Pobell S.** 2011. Bio-precipitation of uranium by

two bacterial isolates recovered from extreme environments as estimated by potentiometric titration, TEM and X-ray absorption spectroscopic analyses. Journal of Hazardous Materials **197:**1-10.

14. **Yung MC, Jiao Y.** 2014. Biomineralization of uranium by PhoY phosphatase activity aids cell survival in *Caulobacter crescentus*. Applied and environmental microbiology.
15. **Poindexter JS.** 1981. The caulobacters: ubiquitous unusual bacteria. Microbiological reviews **45:**123-179.
16. **Hu P, Brodie EL, Suzuki Y, McAdams HH, Andersen GL.** 2005. Whole-genome transcriptional analysis of heavy metal stresses in *Caulobacter crescentus*. Journal of bacteriology **187:**8437-8449.
17. **Bollmann A, Palumbo AV, Lewis K, Epstein SS.** 2010. Isolation and physiology of bacteria from contaminated subsurface sediments. Applied and environmental microbiology **76:**7413-7419.
18. **Utturkar SM, Bollmann A, Brzoska RM, Klingeman DM, Epstein SE, Palumbo AV, Brown SD.** 2013. Draft Genome Sequence for *Caulobacter* sp. Strain OR37, a Bacterium Tolerant to Heavy Metals. Genome announcements **1**.
19. **McAdams HH, Shapiro L.** 2009. System-level design of bacterial cell cycle control. FEBS letters **583:**3984-3991.
20. **Ely B.** 1991. Genetics of *Caulobacter crescentus*. Methods in enzymology **204:**372-384.
21. **Ryan KR, Taylor JA, Bowers LM.** 2010. The BAM complex subunit BamE (*SmpA*) is required for membrane integrity, stalk growth and normal levels of outer membrane β-barrel proteins in *Caulobacter crescentus*. Microbiology **156:**742-756.
22. **Tsai JW, Alley MR.** 2001. Proteolysis of the *Caulobacter* McpA chemoreceptor is cell cycle regulated by a ClpX-dependent pathway. Journal of bacteriology **183:**5001-5007.
23. **Fritz JS, Bradford EC.** 1958. Detection of Thorium and Uranium. Analytical Chemistry **30:**1021-1022.
24. **Hillson NJ, Hu P, Andersen GL, Shapiro L.** 2007. *Caulobacter crescentus* as a whole-cell uranium biosensor. Applied and environmental microbiology **73:**7615-7621.
25. **Miller JH.** 1972. Experiments in molecular genetics. Cold Spring Harbor Laboratory, [Cold Spring Harbor, N.Y.].
26. **Thanbichler M, Shapiro L.** 2006. MipZ, a spatial regulator coordinating chromosome segregation with cell division in *Caulobacter*. Cell **126:**147-162.
27. **Alessi DS, Uster B, Veeramani H, Suvorova EI, Lezama-Pacheco JS, Stubbs JE, Bargar JR, Bernier-Latmani R.** 2012. Quantitative separation of monomeric U(IV) from UO_2 in products of U(VI) reduction. Environmental science & technology **46:**6150-6157.
28. **Schneider CA, Rasband WS, Eliceiri KW.** 2012. NIH Image to ImageJ: 25 years of image analysis. Nature methods **9:**671-675.
29. **Brauner T, Hulser DF, Strasser RJ.** 1984. Comparative measurements of membrane potentials with microelectrodes and voltage-sensitive dyes. Biochimica et biophysica acta **771:**208-216.
30. **Britos L, Abeliuk E, Taverner T, Lipton M, McAdams H, Shapiro L.** 2011. Regulatory response to carbon starvation in *Caulobacter crescentus*. PloS one **6:**e18179.

31. **Justice SS, Hunstad DA, Cegelski L, Hultgren SJ.** 2008. Morphological plasticity as a bacterial survival strategy. Nature Reviews Microbiology **6:**162-168.
32. **Mitra RS, Gray RH, Chin B, Bernstein IA.** 1975. Molecular mechanisms of accommodation in *Escherichia coli* to toxic levels of Cd^{2+}. Journal of Bacteriology **121:**1180-1188.
33. **Demple B, Halbrook J.** 1983. Inducible repair of oxidative DNA damage in *Escherichia coli*. Nature **304:**466-468.
34. **Sezonov G, Joseleau-Petit D, D'Ari R.** 2007. *Escherichia coli* physiology in Luria-Bertani broth. Journal of bacteriology **189:**8746-8749.
35. **Chang IS, Groh JL, Ramsey MM, Ballard JD, Krumholz LR.** 2004. Differential expression of *Desulfovibrio vulgaris* genes in response to Cu(II) and Hg(II) toxicity. Applied and environmental microbiology **70:**1847-1851.
36. **Giotta L, Agostiano A, Italiano F, Milano F, Trotta M.** 2006. Heavy metal ion influence on the photosynthetic growth of *Rhodobacter sphaeroides*. Chemosphere **62:**1490-1499.
37. **VanEngelen MR, Szilagyi RK, Gerlach R, Lee BD, Apel WA, Peyton BM.** 2011. Uranium exerts acute toxicity by binding to pyrroloquinoline quinone cofactor. Environmental science & technology **45:**937-942.
38. **Bird LJ, Coleman ML, Newman DK.** 2013. Iron and copper act synergistically to delay anaerobic growth of bacteria. Applied and environmental microbiology **79:**3619-3627.
39. **Levin BR, Rozen DE.** 2006. Non-inherited antibiotic resistance. Nature reviews. Microbiology **4:**556-562.
40. **Mukherjee A, Wheaton GH, Blum PH, Kelly RM.** 2012. Uranium extremophily is an adaptive, rather than intrinsic, feature for extremely thermoacidophilic *Metallosphaera* species. Proceedings of the National Academy of Sciences of the United States of America **109:**16702-16707.
41. **Yung MC, Ma J, Salemi MR, Phinney BS, Bowman GR, Jiao Y.** 2014. Shotgun Proteomic Analysis Unveils Survival and Detoxification Strategies by Caulobacter crescentus during Exposure to Uranium, Chromium, and Cadmium. Journal of proteome research **13:**1833-1847.
42. **Gorbatyuk B, Marczynski GT.** 2005. Regulated degradation of chromosome replication proteins DnaA and CtrA in *Caulobacter crescentus*. Molecular microbiology **55:**1233-1245.
43. **Quon KC, Yang B, Domian IJ, Shapiro L, Marczynski GT.** 1998. Negative control of bacterial DNA replication by a cell cycle regulatory protein that binds at the chromosome origin. Proceedings of the National Academy of Sciences of the United States of America **95:**120-125.
44. **Laub MT, Chen SL, Shapiro L, McAdams HH.** 2002. Genes directly controlled by CtrA, a master regulator of the *Caulobacter* cell cycle. Proceedings of the National Academy of Sciences of the United States of America **99:**4632-4637.
45. **Markich SJ, Brown PL, Jeffree RA, Lim RP.** 2000. Valve movement responses of *Velesunio angasi* (Bivalvia: Hyriidae) to manganese and uranium: an exception to the free ion activity model. Aquatic toxicology **51:**155-175.
46. **Ebbs SD, Brady DJ, Kochian LV.** 1998. Role of uranium speciation in the uptake and translocation of uranium by plants. Journal of Experimental Botany **49:**1183-1190.
47. **Khemiri A, Carriere M, Bremond N, Ben Mlouka MA, Coquet L, Llorens I, Chapon V, Jouenne T, Cosette P, Berthomieu C.** 2014. *Escherichia coli*

Response to Uranyl Exposure at Low pH and Associated Protein Regulations. Plos One **9**.

Figure Legends

Figure 1. U(VI)-induced growth arrest in *C. crescentus*. (A) Cell growth with U(VI) added at the beginning of incubation. Error bars represent the standard deviation of three biological replicates. (B) The effect of inoculum size on growth arrest duration with 300 μM U(VI). Data represent the average of two biological replicates that varied by less than 20%. (C) CFU measurements during growth in the presence of U(VI). Error bars represent the standard deviation of three biological replicates.

Figure 2. Comparison of growth arrest duration for *Caulobacter crescentus*, *Escherichia coli* K12, *Pseudomonas aeruginosa* PAO1, and *Pseudomonas putida* KT2440. Growth curves with no U(VI) (A) and with 350 μM U(VI) (B). Data represent the average of two biological replicates that varied by less than 30%.

Figure 3. Adaptive changes of *C. crescentus* following exposure to 350 μM U(VI). (A) Representative SEM images of cells collected at different time points during growth in the presence of U(VI). The time following U(VI) addition and the growth stage of cells are indicated above each image. Scale bar, 1 μm. (B) Representative SEM images after exposure of synchronized swarmer cells to U(VI). The time following U(VI) addition and the growth stage of cells are indicated above each image. Scale bar, 1 μm. (C) Replication initiation following U(VI)-induced growth arrest was visualized in a synchronized population containing a chromosomal *ecfp-parB* fusion. The percentage of the population with two ParB-CFP foci at each time point is indicated. Top panels: DIC, bottom panels: ParB-CFP fluorescence. (D) Control depicting ParB-CFP foci after one hour of growth in media lacking U(VI). (E) ParB-CFP foci within representative filamentous cells shortly after growth recovery (OD_{600} of 0.15).

Figure 4. The sensitivity of *C. crescentus* to repeated U(VI) exposure. (A) Cells grown on PYE agar containing either 0, 500 or 700 μM U(VI) (labeled at top of image) were re-spotted on PYE agar containing 0, 500 or 700 μM U(VI) (labeled at bottom of image). The spotting represents 10-fold serial dilutions (10^0 to 10^6), ordered from top to bottom. Results are representative of three replicates. (B) Cells grown to mid-exponential phase in PYE containing 0 (open symbol) or 350 μM (filled symbol) U(VI) were re-inoculated into fresh PYE containing 350 μM U(VI) and growth was monitored.

Figure 5. Cell-mediated reduction in U(VI) toxicity by *C crescentus* during growth arrest. (A) Supernatant from live cells ($5.4x10^7$ cells/ml), heat killed cells ($5.4x10^7$ cells/ml), and an abiotic control was collected prior to the end of growth arrest and used as growth medium for re-inoculation. Growth in fresh medium with or without 350 μM U(VI) (open symbols) are shown for comparison. Data represent the average of two biological replicates that varied by less than 30%. (B) Supernatant from growth arrested cultures (bottom tract) was collected every ~75 min (roman numerals) and used as growth medium for re-inoculation. Growth time (top tract) represents the length of time for the re-inoculated culture to reach an OD_{600} of 0.2. The dashed line represents the growth time for cells inoculated in a medium lacking U(VI) (*i.e.*, no growth inhibition). The growth time in supernatant collected from an abiotic control is shown for comparison. Error bars represent the standard deviation of three biological replicates. (C) Time course of P_{urcA}-*lacZ* expression (top panel) at different U(VI) concentrations. The growth curve at each U(VI) concentration is displayed on the bottom tract for reference.

Figure 6. The reduction of U(VI) toxicity through modulation of growth medium pH (A). Measurement of medium pH during growth of *C. crescentus* with 350 μM U(VI). Data represent the average of two biological replicates that varied by less than 10%. (B) Effect of pH adjustment of the medium on growth arrest duration. The pH of PYE containing 350 μM U(VI) (pH 5.7) was adjusted to 6.1 (open symbol) prior to inoculation.

Data represent the average of two biological replicates that varied by less than 20%. (C) Effect of pH adjustment on P_{urcA}-*lacZ* expression during growth arrest induced by 350 μM U(VI). Plot symbols are the same as in (B). (D) Measurement of medium pH during growth of *P. aeruginosa*, *P. putida* and *E. coli* with U(VI). The concentrations of U(VI) used are 350 μM, 175 μM, and 90 μM for *P. aeruginosa*, *P. putida* and *E. coli,* respectively. pH is plotted on the top tract while OD_{600} is plotted on the bottom tract. Data represent the average of two biological replicates that varied by less than 10%. (E) The soluble (closed symbols) and total (open symbols) concentrations of U(VI) measured during growth of *C. crescentus* with 350 μM U(VI). The dashed line marks the time when growth recovery occurred.

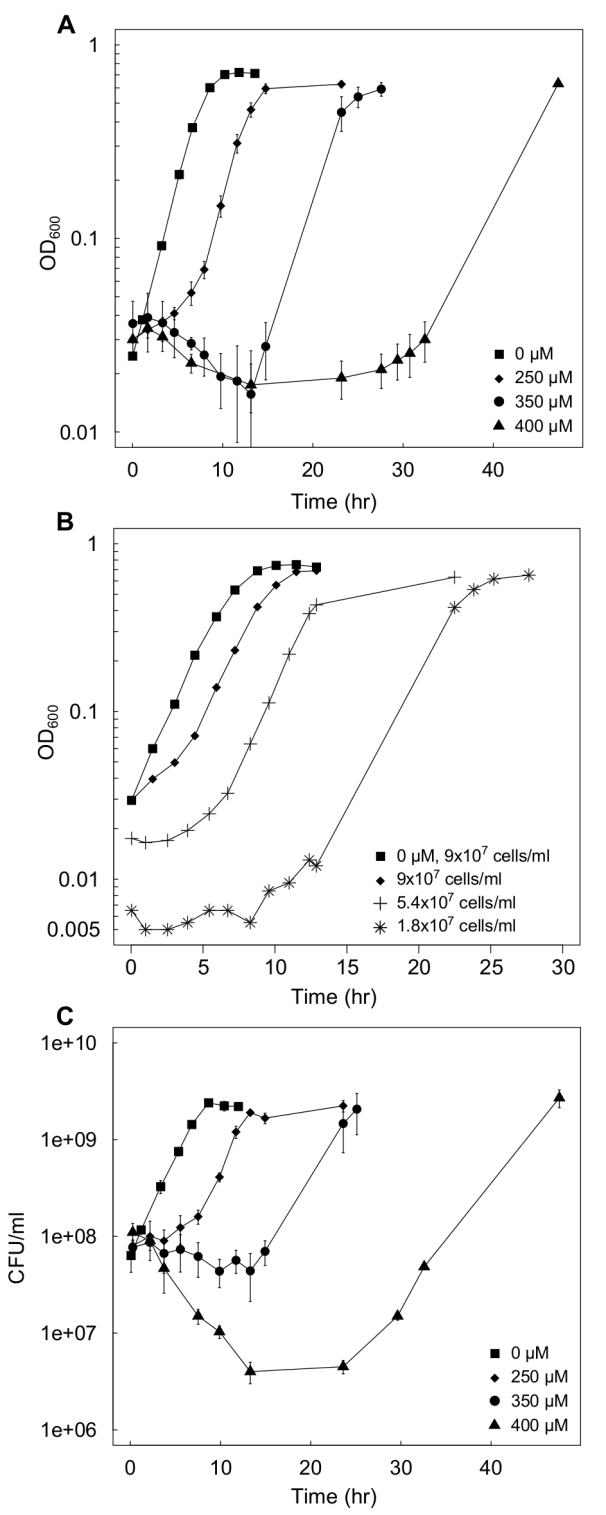
A
1
0.1
0.01
OD600
0
10
20
30
40
Time (hr)
0 μM
250 μM
350 μM
400 μM
B
1
0.1
0.01
0.005
OD600
0
5
10
15
20
25
30
Time (hr)
0 μM, 9x10^7 cells/ml
9x10^7 cells/ml
5.4x10^7 cells/ml
1.8x10^7 cells/ml
C
1e+10
1e+09
1e+08
1e+07
1e+06
CFU/ml
0
10
20
30
40
Time (hr)
0 μM
250 μM
350 μM
400 μM

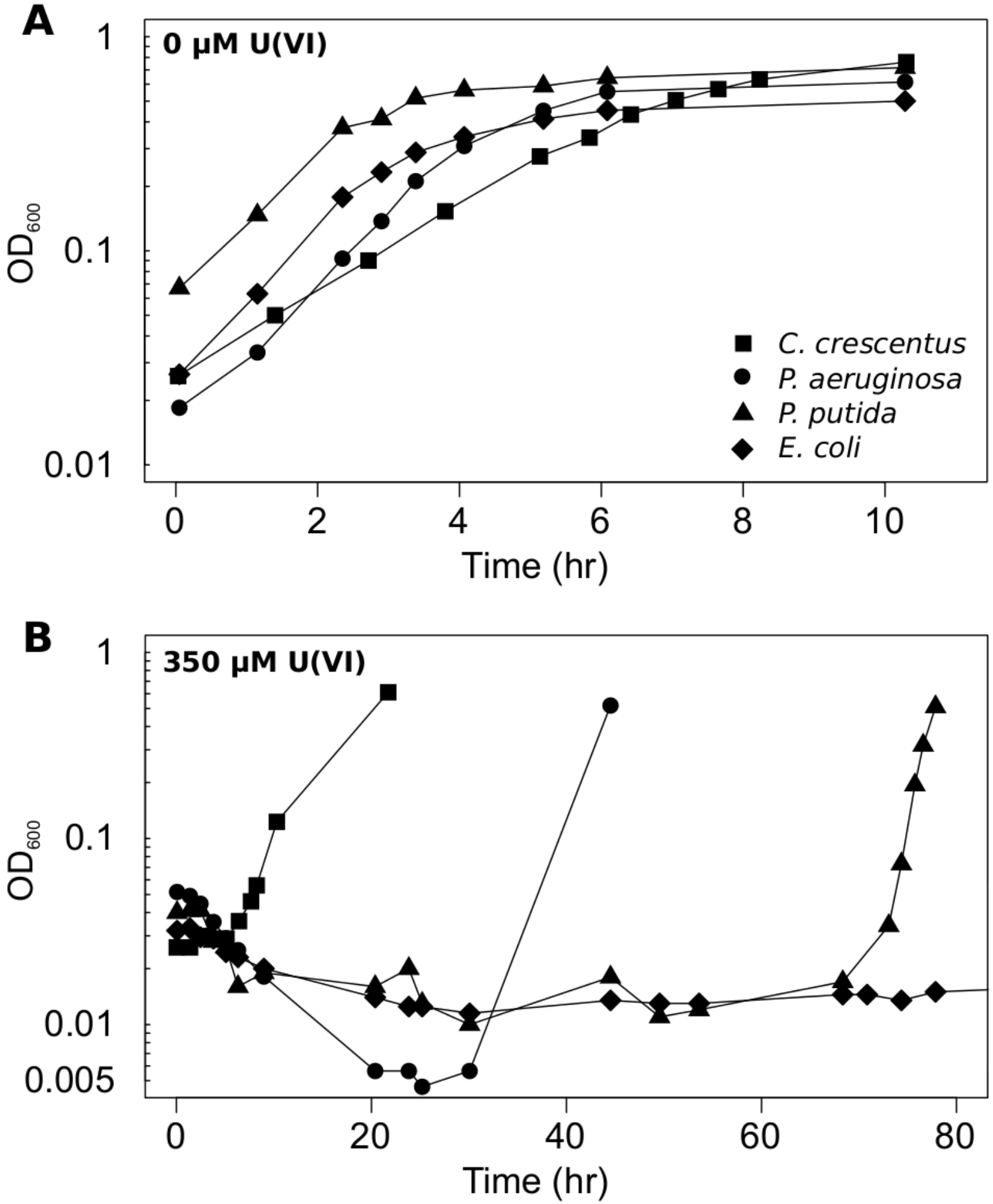
A
0 μM U(VI)
1
0.1
0.01
OD600
C. crescentus
P. aeruginosa
P. putida
E. coli
0
2
4
6
8
10
Time (hr)
B
350 μM U(VI)
1
0.1
0.01
0.005
OD600
0
20
40
60
80
Time (hr)

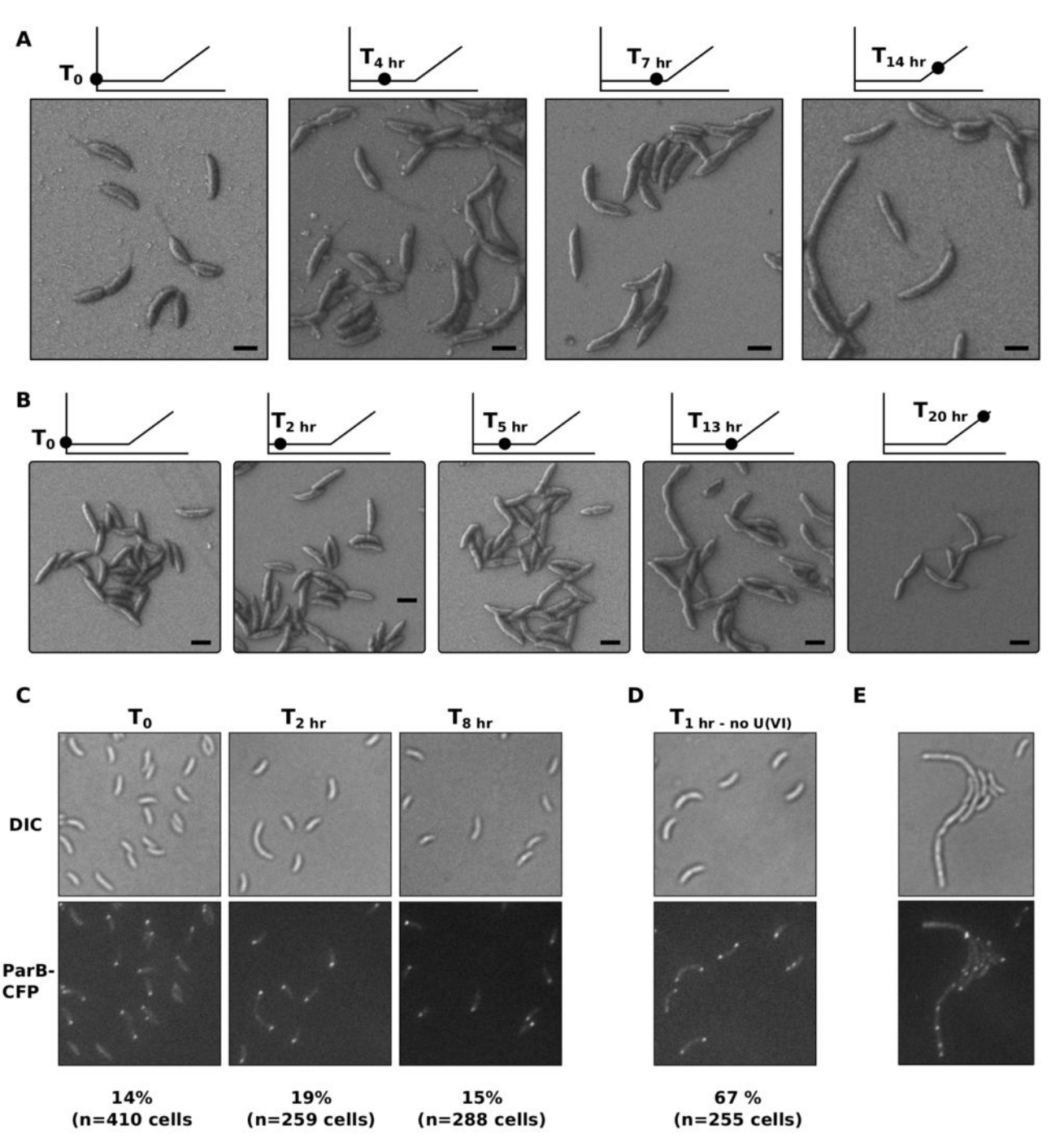
A
T0
T4 hr
T7 hr
T14 hr
B
T0
T2 hr
T5 hr
T13 hr
T20 hr
C
T0
T2 hr
T8 hr
DIC
ParB-CFP
14%
(n=410 cells
19%
(n=259 cells)
15%
(n=288 cells)
D
T1 hr - no U(VI)
67 %
(n=255 cells)
E

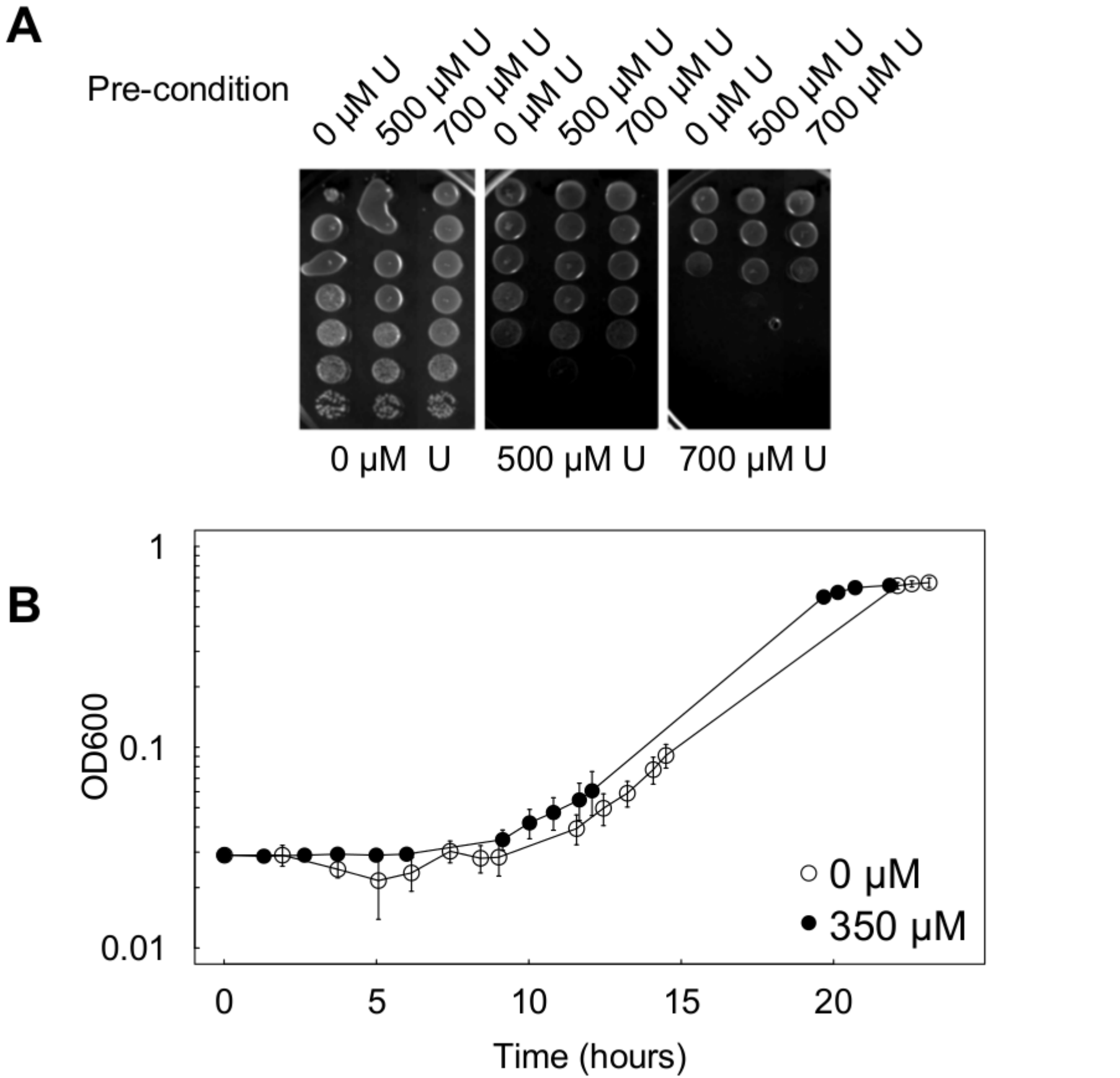
A
Pre-condition
0 μM U
500 μM U
700 μM U
0 μM U
500 μM U
700 μM U
0 μM U
500 μM U
700 μM U
0 μM U
500 μM U
700 μM U
B
OD600
1
0.1
0.01
0
5
10
15
20
Time (hours)
0 μM
350 μM

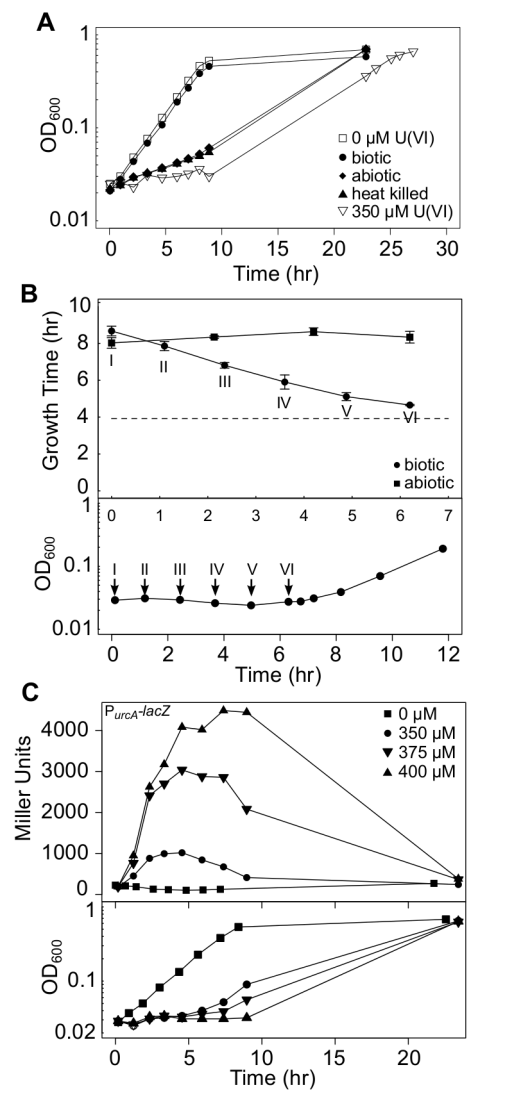
A
OD600
1
0.1
0.01
0 μM U(VI)
biotic
abiotic
heat killed
350 μM U(VI)
0 5 10 15 20 25 30
Time (hr)
B
Growth Time (hr)
10 8 6 4 2 0
I II III IV V VI
biotic
abiotic
0 1 2 3 4 5 6 7
OD600
1 0.1 0.01
I II III IV V VI
0 2 4 6 8 10 12
Time (hr)
C
PurcA-lacZ
Miller Units
4000 3000 2000 1000 0
0 μM
350 μM
375 μM
400 μM
OD600
1 0.1 0.02
0 5 10 15 20
Time (hr)

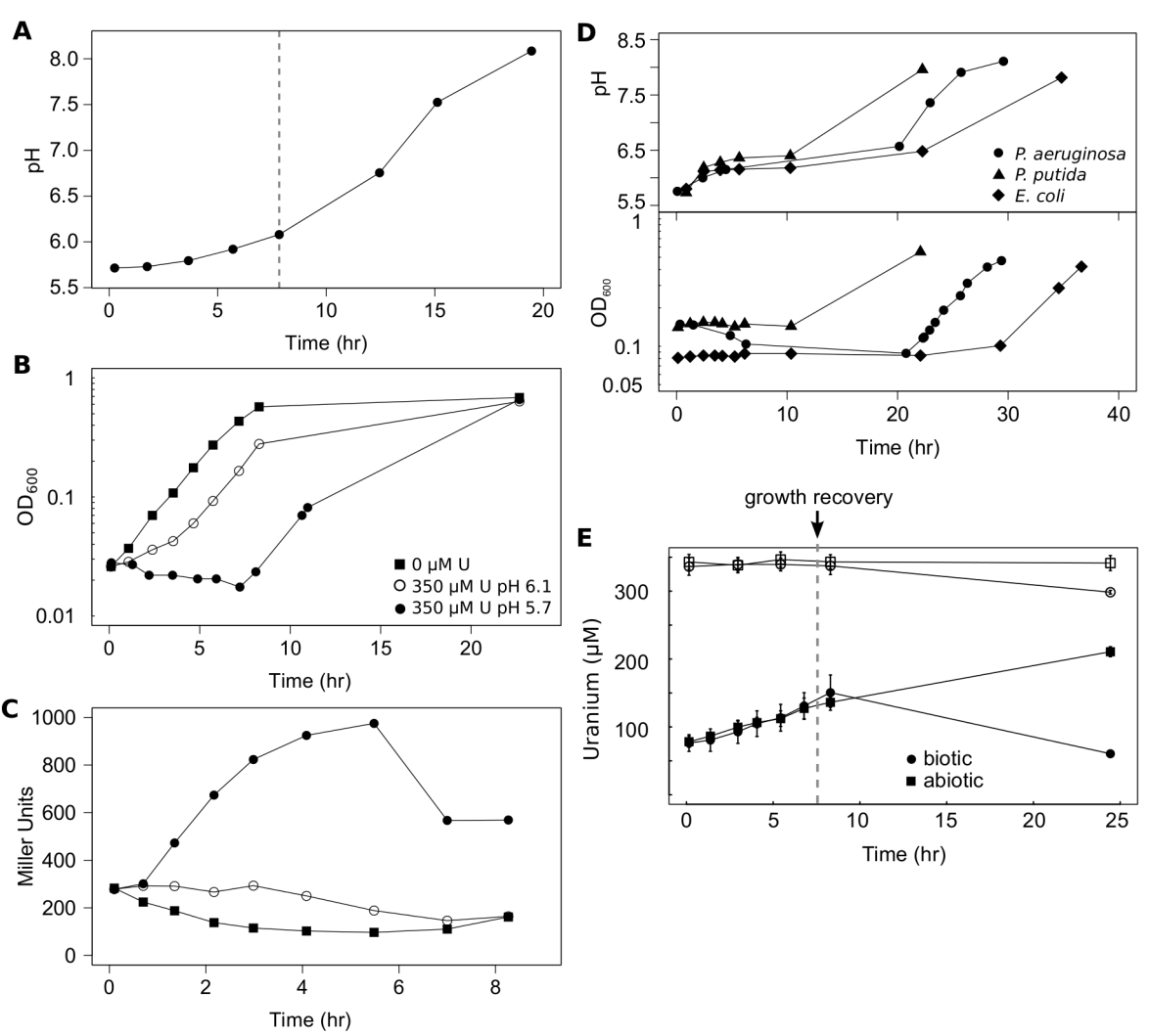
A
pH
Time (hr)
B
OD600
0 μM U
350 μM U pH 6.1
350 μM U pH 5.7
Time (hr)
C
Miller Units
Time (hr)
D
pH
P. aeruginosa
P. putida
E. coli
OD600
Time (hr)
E
growth recovery
Uranium (μM)
biotic
abiotic
Time (hr)

Modulation of medium pH by *Caulobacter crescentus* facilitates recovery from uranium-induced growth arrest

Dan M. Park[1], Yongqin Jiao[1]*

Supplemental Material

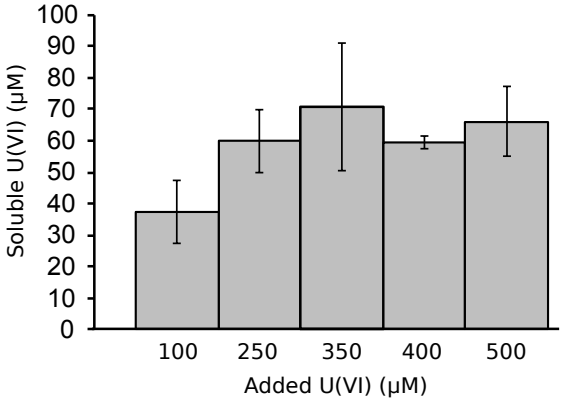

Figure S1. Solubility of U(VI) in PYE at different added U(VI) concentrations. Error bars represent the standard deviation of three biological replicates.

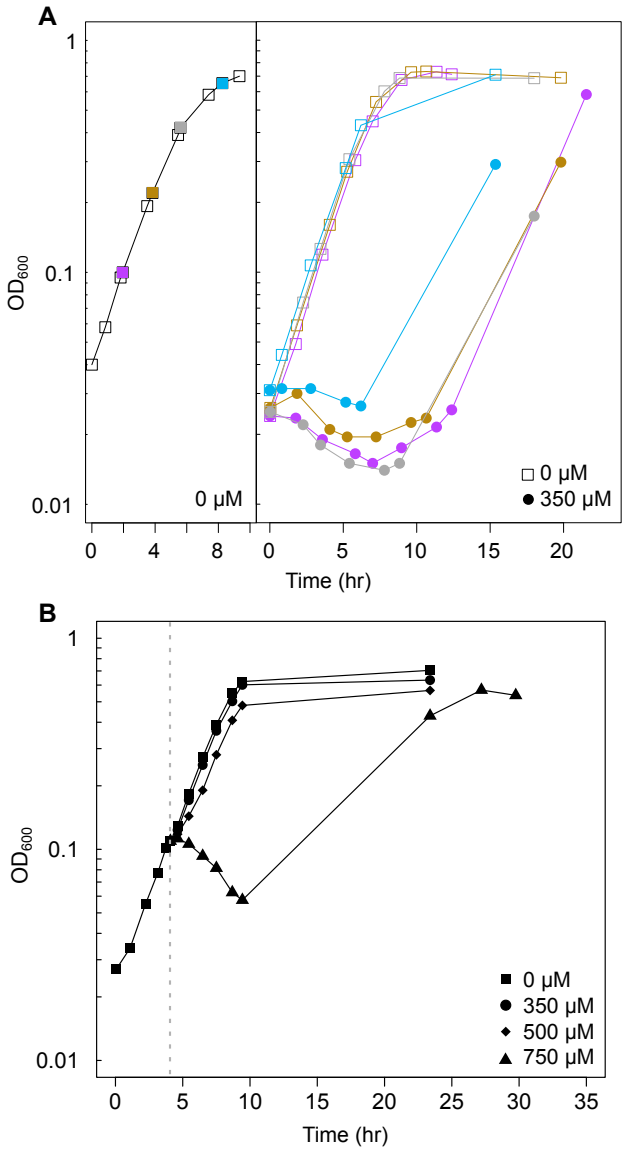

Figure S2. Characterization of *Caulobacter* growth during U(VI) exposure. (A) Cells collected from different growth phases (left panel) were inoculated into PYE with (closed symbols) or without (open symbols) 350 μM U(VI) and growth was monitored by OD_{600} (right panel). The growth phase of each inoculum is denoted by a filled square that is color coded with the corresponding growth curve. (B) U(VI) was added at early exponential phase (OD_{600} of 0.1, corresponding to $3.3x10^8$ cells/ml). The dashed gray line depicts the time of U(VI) addition. A control of HNO_3 (to 750 μM) alone did not perturb growth, suggesting that the growth arrest was caused by uranyl nitrate. Data represent the average of two biological replicates that varied by less than 10%.

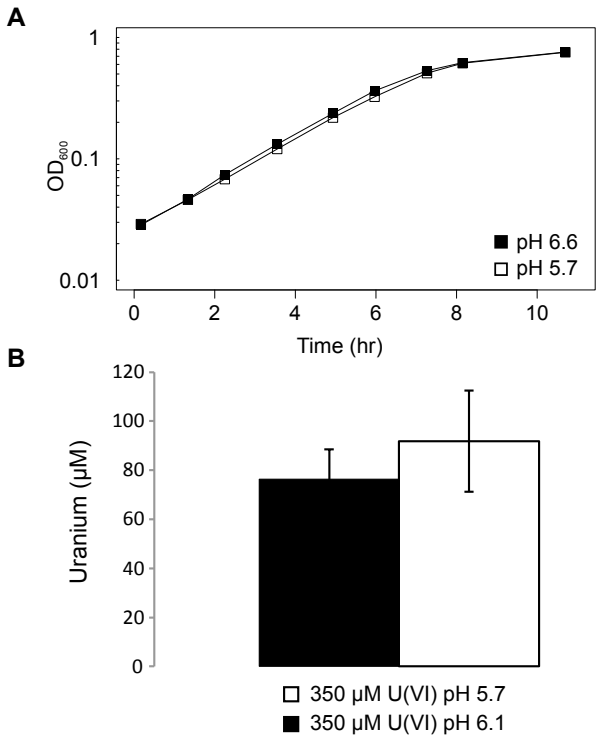

Figure S3. The effect of pH on *Caulobacter* growth and U(VI) solubility. (A) Growth curves at pH 5.7 (pH of PYE with 350 μM U(VI)) and pH 6.6 (pH of PYE) overlap in the absence of U(VI). Data represent the average of two biological replicates that varied by less than 10%. (B) Soluble U(VI) concentration in PYE at pH 5.7 and 6.1 (pH at the end of growth arrest). Error bars represent the standard deviation of three biological replicates.

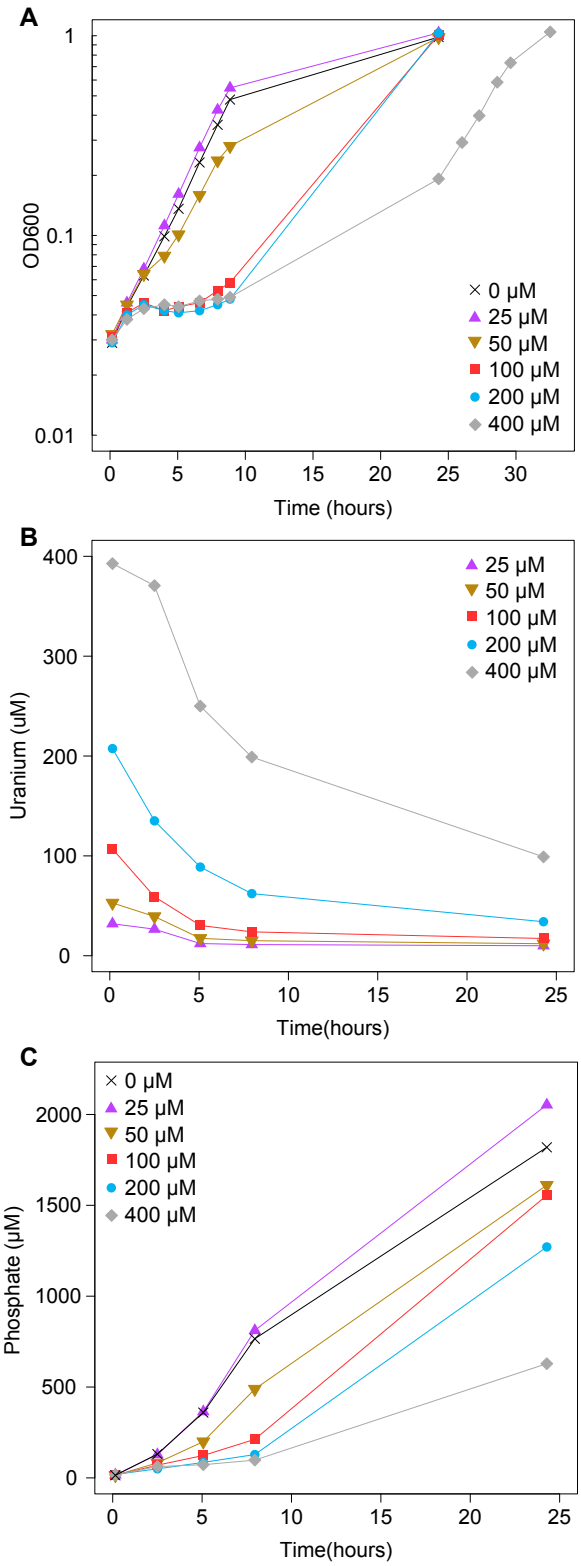

Figure S4. U(VI)-induced growth arrest of *Caulobacter* in M5G-G2P medium. (A) Cell growth in the presence of U(VI). (B) Soluble U(VI) concentration during growth in U(VI).

(C) Soluble inorganic phosphate concentration during growth in U(VI). U(VI) concentrations tested are indicated in the figure legends.

Supplemental Tables

Table S1. Cell dry weight determination of the bacterial species tested.

Species	Cell dry weight (g/cell)[a]
C. crescentus	5.3×10^{-11}
E. coli	6.0×10^{-11}
P. putida	1.3×10^{-10}
P. aeruginosa	1.1×10^{-10}

[a]Determined from cells harvested at an OD_{600} of 0.5.